applied sciences

MDPI

Article

An Experiment Study on the Dynamic Behavior of Concrete Used in a Mine Sealing Wall under a High Temperature

Qiusha Wang * and Zhenmin Luo

College of Safety Science and Engineering, Xi'an University of Science and Technology, Xi'an 710054, China
* Correspondence: 004015@xust.edu.cn

Abstract: Micro-cracks and material deterioration occur in concrete under high-temperature conditions. To reveal the impact resistance of concrete at a high temperature, a dynamic splitting test and dynamic compression test were carried out using a split Hopkinson pressure bar (SHPB). The failure process and dynamic stress–strain curve of the concrete specimens were obtained, investigating the failure mode and dynamic tensile and compressive strength of the concrete. The test results showed that the surface cracks appeared along the loading direction and extended to the core area under the impact load. With an increase in the temperature, different degrees of damage would be caused, the dynamic strength and toughness of the concrete would decrease, showing brittle failure, and the energy absorbed in the failure process would also decrease correspondingly.

Keywords: high temperature; concrete used in mine sealing wall; SHPB; dynamic behavior; dissipation of energy

1. Introduction

There are a large number of crossheadings designed in the coal mine production process, which need to be closed in the process of continuous excavation. When the working face is exposed to fire, it is difficult to effectively control it in a short time, and the fire area can be closed for isolation and fire suppression [1]. A high-strength fireproof fiber flexible mold bag filled with inorganic curing material has the advantages of a high strength, good durability, and being flame retardant, and the inorganic curing material filled in the mold bag is mainly concrete [2–4]. Flexible film bags are widely used in roadway support [5,6], gob filling [7,8], fire control in roadways [9,10], and so on. It is easy to induce a gas explosion with fire in coal roadways, and the sealing wall of the crossheading and temporary sealing wall of the fire area will bear the coupling effect of the high temperature and explosion shock [11]. It is necessary to study the dynamic behavior of concrete at a high temperature in order to improve the impact resistance of the sealing wall. At present, research on sealing walls is mainly carried out through numerical simulations to study their antiknock performance [12–14]. Most researchers focus on the dynamic compressive properties of materials after high temperatures and cooling [15–20]. Su, Li, and Chen et al., respectively, designed a high-temperature dynamic loading device to explore the dynamic compression characteristics of concrete at a high temperature [21–23]. Yu et al., used the yield criterion in exponential form and associated flow rule to describe the plastic characteristics of concrete at a high temperatures [24]. Jin et al., investigated the dynamic compression failure behavior and dynamic splitting behavior of concrete at a high temperature and its microscopic damage mechanism [25,26]. Li et al., investigated the dynamic compression behavior of concrete-filled steel tubes under single and multiple impacts using a split Hopkinson pressure bar (SHPB) [27]. Su et al., researched the dynamic compressive strength of concrete at different temperatures using a self-developed heating device [21]. Chen et al., conducted high-temperature and high-strain-rate tests on ordinary concrete using an SHPB test device and self-developed industrial microwave heating

Citation: Wang, Q.; Luo, Z. An Experiment Study on the Dynamic Behavior of Concrete Used in a Mine Sealing Wall under a High Temperature. *Appl. Sci.* **2023**, *13*, 9339. https://doi.org/10.3390/app13169339

Academic Editor: Ricardo Castedo

Received: 18 July 2023
Revised: 8 August 2023
Accepted: 14 August 2023
Published: 17 August 2023

furnace, and discussed the influence of the temperature and strain rate on the mechanical properties of the concrete materials [23]. In addition, Wang, Li, and Zhang et al., conducted high-temperature dynamic loading tests on concrete materials to explore the dynamic damage performance and failure mode of the concrete [28–30].

Concrete composites used in mines are susceptible to catastrophic failure under intense, sudden blasts or explosions. These types of structure must be rendered less susceptible to failure through the adoption of materials with a high energy absorption capacity [31]. Liu et al., revealed the damage and failure mechanism of concrete in mines from the perspective of energy and damage [32]. Yang et al., carried out an SHPB impact test and numerical simulation on plain concrete and fiber-reinforced concrete, and the total energy consumption of the concrete increased with the increase in the strain rate [33]. Feng et al., defined the damage sensitivity of energy absorption, which links the dynamically imposed energy, overall damage, and fragmentation distribution, and reveals the energy absorption characteristics of foamed concrete [34]. Liu et al., carried out a series of drop-weight impact tests on concrete, and analyzed the developments of impact force, strain, the contact stress–strain relationship, and absorbed energy during the drop-weight impact test [35]. In impact tests, the energy consumption is a comprehensive reflection of strength and ductility. The dynamic properties of concrete can be further revealed from the perspective of energy.

However, dynamic tests on concrete materials at a high temperature are all based on temperature gradient, and the overall heating method is used to study the dynamic characteristics. In this paper, only one side of the mine sealing wall is placed in the high-temperature condition, and the concrete specimen is heated on one side to study its impact resistance at different temperatures, which provides a basis for the design of the filling thickness and location of the sealing walls in crossheadings.

2. Materials and Methods

2.1. Materials

According to the actual requirements of mine crossheadings that are explosion-proof and fireproof [36], the designed mix ratio of concrete is shown in Table 1. Using P.O. 42.5 grade normal Portland cement, the fineness modulus of sand was 2.92 and the particle size of stone was 5~15 mm. In order to improve the fluidity, strength, and shrinkage of concrete, a magnesium aluminosilicate suspension agent, polycarboxylic acid reinforcement agent, and UEA expansion agent were added. The concrete mixture was accurately weighed, mixed with water, and vibrated on a shaking table. The specimens were placed in standard curing equipment with a constant temperature (20 ± 2 °C) and humidity (95%) for 28 d. The specimens with a curing age of 28 d were treated with high temperatures at 20 °C, 100 °C, 200 °C, 300 °C, and 400 °C, and dynamic impact tests were carried out. In order to ignore the influence of the axial and transverse inertia effects of the specimen [37] and consider the diameter of the pressure rod of the test equipment, the specimen size for the dynamic impact test was a cylindrical specimen with a diameter of 75 mm and height of 50 mm. The prepared specimens are shown in Figure 1. Before the test, the end faces of the specimens were polished to ensure that the flatness and parallelism of the end met the requirements of the test. High-grade lubricants were applied on both ends of the specimens to reduce the adverse effects of friction.

Table 1. Mix proportion of concrete (unit: kg·m^{-3}).

Cement	Sand	Stone	Suspension Agent	Reinforcement Agent	Expansion Agent
350	600	1550	10	5	3.5

Figure 1. Concrete specimens.

2.2. SHPB Test

According to the temperature change law of the sealing wall in the closed fire area [11], one side of the test specimens was heated using a stainless steel electric heating plate (DB-1AB), and 5 temperature conditions, including 20 °C, 100 °C, 200 °C, 300 °C, and 400 °C, were set, respectively. When the heating plate reached the target temperature, the temperature was maintained for 2 h. The heating system's power was 1.8 kW, as shown in Figure 2. At each temperature condition, the concrete specimens under constant temperature conditions for 2 h were subjected to a dynamic impact test. The impact load of the compressive test was 0.1 MPa, and the impact load of the splitting test was 0.08 MPa. In the impact test, an SHPB with a diameter of 76 mm was adopted, as shown in Figure 3. The SHPB system consisted of a striker, input bar, output bar, stoper, and monitoring equipment. By attaching strain gauges to the input bar and output bar, a dynamic strain gauge was used to collect the dynamic waveform data of the specimen, and the test data were converted into the stress–strain curve of the specimen. During the dynamic impact test, a pre-impact test was carried out on the specimen, and three repeated tests were carried out under the same working conditions. The average of the three groups of effective data was selected as the test result.

Figure 2. Heating system.

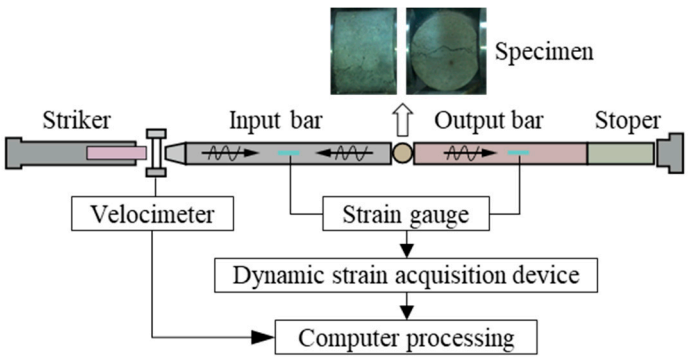

Figure 3. SHPB loading system.

3. Test Results and Discussion

3.1. Failure Mode

In order to reveal the progressive failure process of concrete specimens under impact load, the failure modes of the concrete specimens during an impact splitting test and impact compression were recorded using a high-speed camera.

3.1.1. Dynamic Splitting Test

Under the impact splitting load, the failure process of the concrete specimen is shown in Figure 4. In the process of the impact splitting test, the specimen was slightly damaged at the loading point first under the splitting load. With an increase in the load, the damage zone of the specimen extended from the loading points on both sides to the center, and a penetrating crack was formed in the loading direction. A triangular crushing zone was formed at the loading point of the input bar or the output bar. The reason for the different positions of the crushing zone was the difference between the loading boundary of the splitting test and the internal structure of the specimen. Under the continuous action of the impact load, the triangular crushing zone gradually expanded along the central crack, and the specimen was pulled and split into two parts, as shown in Figure 5, and part of the concrete block was crushed. After a high-temperature treatment, the specimen showed brittle failure. The concrete specimens treated at 300 °C and 400 °C were finally crushed under the impact splitting load, and the specimens were broken into fine blocks.

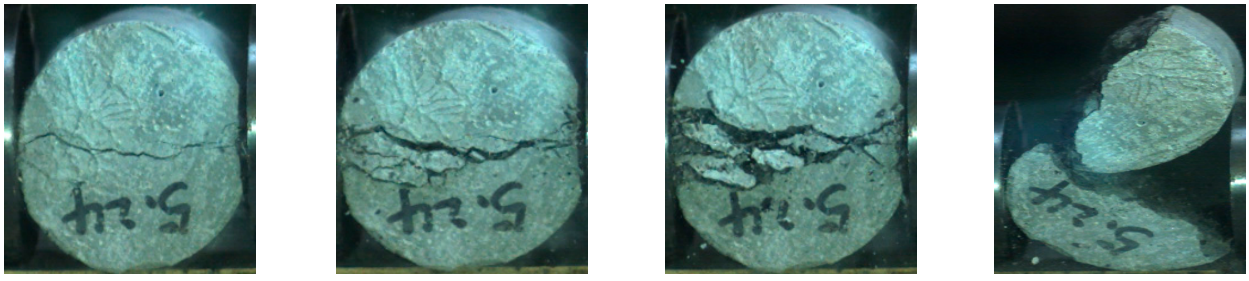

(**a**)

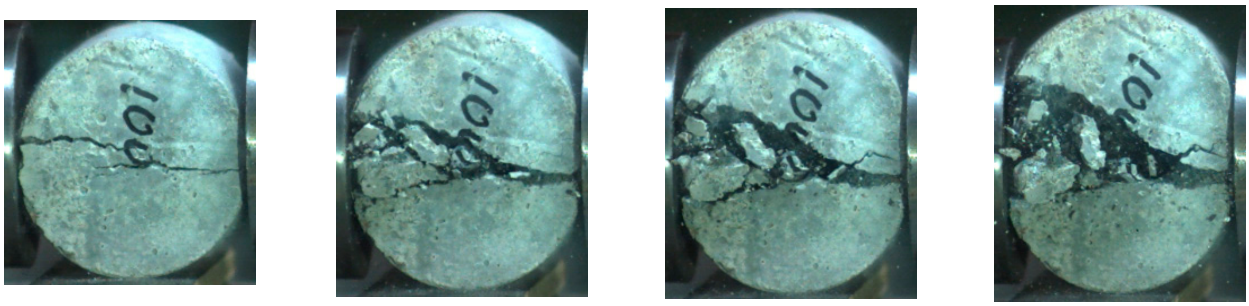

(**b**)

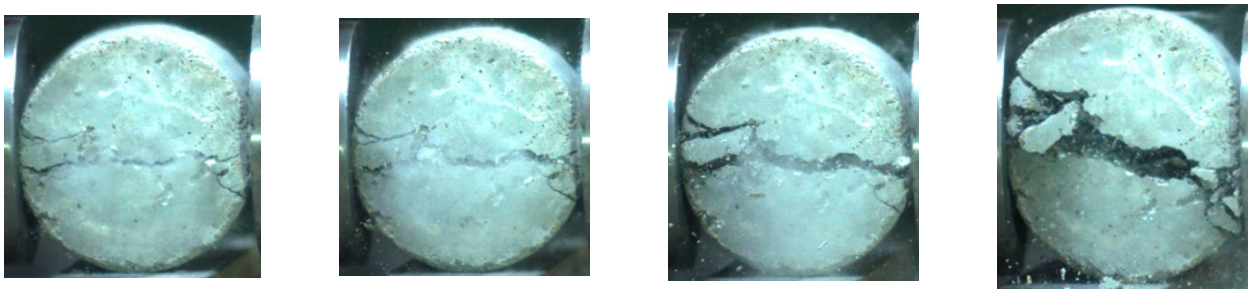

(**c**)

Figure 4. *Cont.*

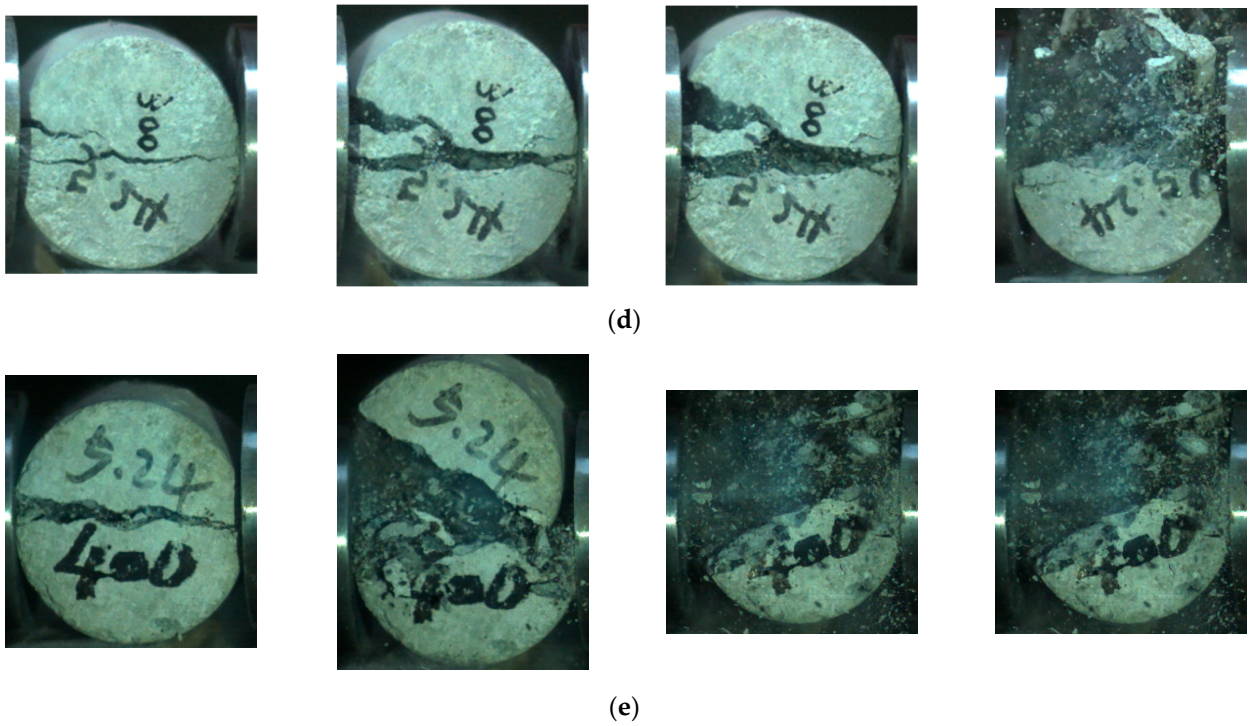

Figure 4. Failure modes of concrete specimens at different temperatures: (**a**) 20 °C; (**b**) 100 °C; (**c**) 200 °C; (**d**) 300 °C; and (**e**) 400 °C.

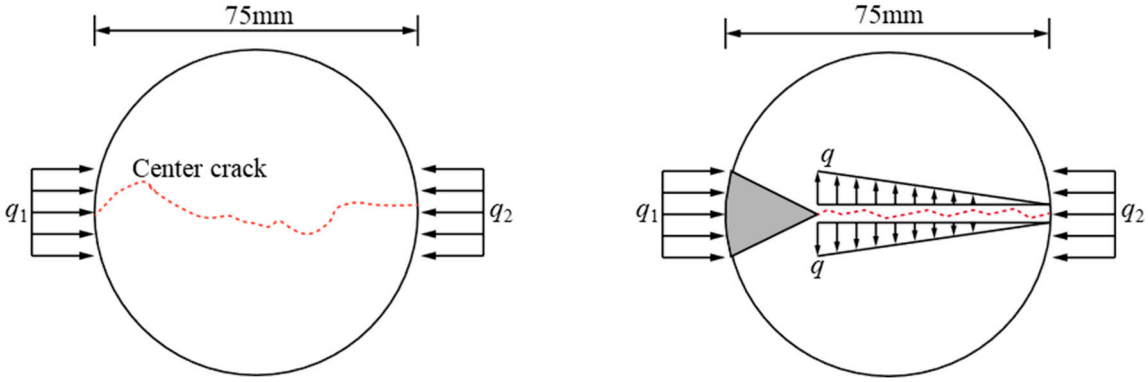

Figure 5. Failure model of specimen: (**a**) center crack of specimen; and (**b**) crack expansion mode of specimen.

3.1.2. Dynamic Compressive Test

The failure mode of the concrete specimen under the impact load is shown in Figure 6. At the initial stage of loading, the specimen was damaged from the edge and cracks appeared on the surface. The direction of the cracks was consistent with the direction of the loading. With the increase in the load, micro-cracks developed and merged, resulting in the surface block of the specimen falling off and the main cracks developing towards the core concrete. When the impact load was transmitted in the specimen, the crack spread along the loading direction. Due to the Poisson effect, the specimen exhibited axial splitting failure. In the failure stage, as the impact load continued to increase, the concrete specimen continued to absorb energy, forming micro-cracks inside the specimen, and the concrete specimen finally broke into small pieces along the main crack. However, under the impact load, the specimen treated at 400 °C only broke into three large blocks, showing significant brittle failure and a decreasing impact toughness.

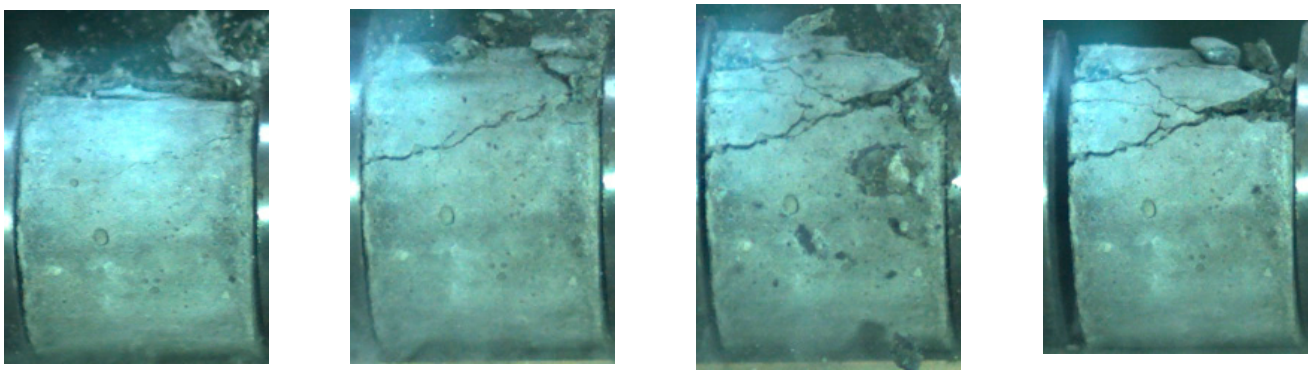

(**a**)

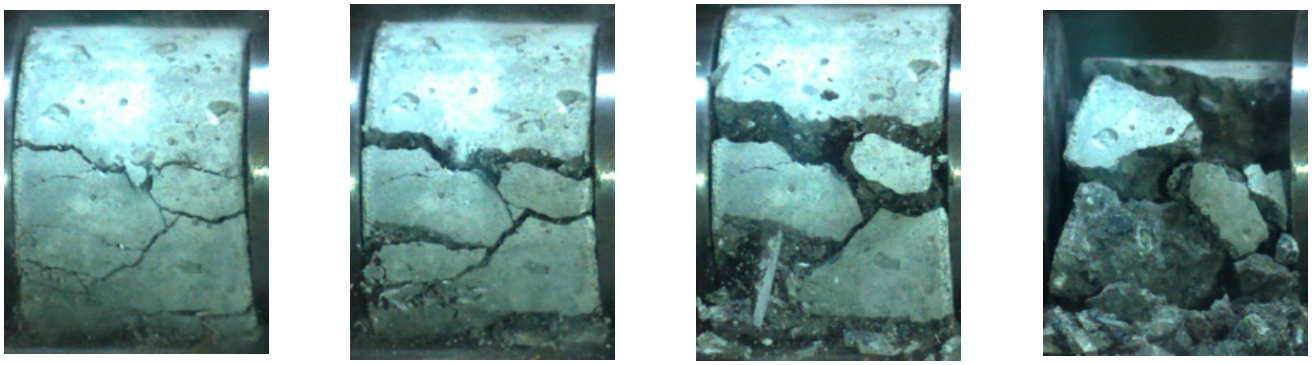

(**b**)

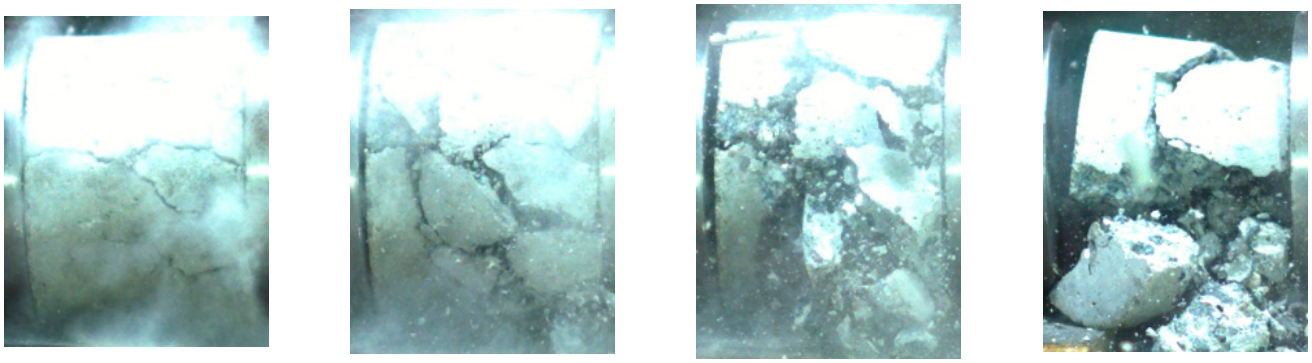

(**c**)

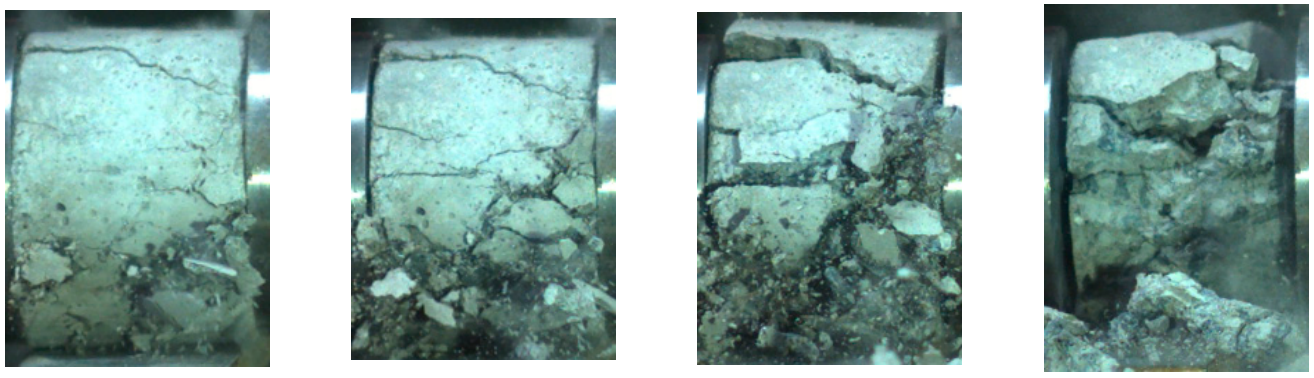

(**d**)

Figure 6. *Cont*.

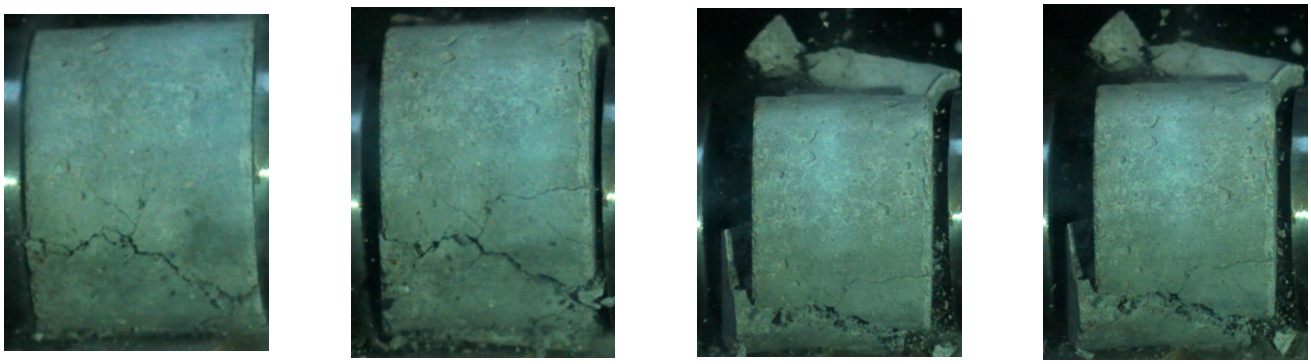

(**e**)

Figure 6. Failure modes of concrete specimens under compression at different temperatures: (**a**) 20 °C; (**b**) 100 °C; (**c**) 200 °C; (**d**) 300 °C; and (**e**) 400 °C.

3.2. Dynamic Stress–Strain Characteristics

3.2.1. Dynamic Splitting Test

Under the impact load, the dynamic stress–strain curves of the specimens treated at different temperatures are shown in Figure 7. The dynamic splitting strength is the peak stress on the curve, which is one of the important indexes for reflecting the impact resistance of concrete. At the initial stage of loading, the curve increased linearly, and the specimen was in the elastic stage. When the impact load reached the splitting tensile strength of the specimen, the peak strain of the specimen was about 0.5%, many small micro-cracks appeared, the concrete in the loading area was crushed, and the specimen was damaged. With the increase in the load, the strength of the specimen decreased sharply, the cracks penetrated rapidly, many split concrete blocks were crushed, and the structure of the specimen was damaged. The dynamic splitting tensile strength curves of the concrete specimens at different temperatures are shown in Figure 8. At 100 °C, 200 °C, 300 °C, and 400 °C, the dynamic splitting tensile strengths of the specimens were 80.34%, 74.93%, 65.81%, and 62.96% of the normal temperature, respectively. After the action of the high temperature, micro-cracks in the matrix structure appeared and the material deteriorated, resulting in the dynamic splitting tensile strength of the concrete gradually decreasing with the temperature. At the same time, the peak strain of the specimen also showed a decreasing trend. After the high-temperature treatment, the toughness of the concrete decreased significantly, so the specimen showed brittle failure in the failure stage.

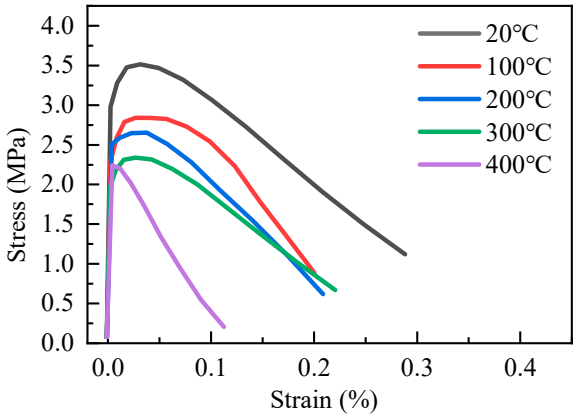

Figure 7. Dynamic stress–strain curve of specimens in dynamic splitting test.

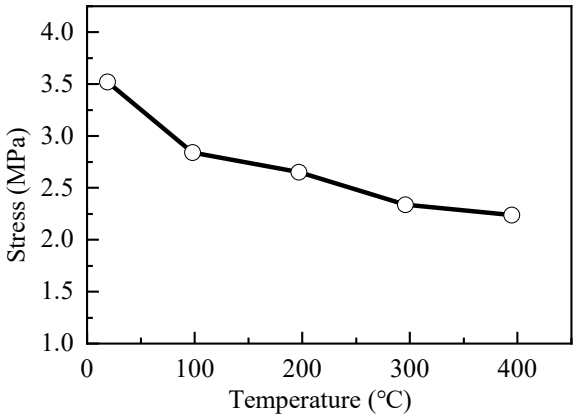

Figure 8. Dynamic splitting tensile strength at different temperature.

3.2.2. Dynamic Compressive Test

Under the impact load, the dynamic compressive stress–strain curves of the concrete specimens treated at different temperatures are shown in Figure 9. At the initial stage of loading, the stress–strain curve increased linearly, the specimens were in the elastic stage, and quickly reached the compressive strength of the specimens. The elastic modulus of the specimens treated at different temperatures was basically the same. With the increase in the impact load, the stress of the specimens decreased gradually. When the strain was about 0.4%, the stress of the specimen had a minimum value, then a small increase, and finally presented a plastic flow until failure. The dynamic compressive strength change curves of the specimens treated at different temperatures are shown in Figure 10. The dynamic compressive strengths of the specimens at 100 °C, 200 °C, 300 °C, and 400 °C were 86.04%, 81.74%, 78.69%, and 67.21% of the normal temperature, respectively. With the increase in the temperature, the peak stress decreased significantly. During the heating process, the free water and partially bound water inside the concrete produced water vapor pressure, which caused micro-cracks and the concrete to be strained, resulting in concrete damage and a decline in the axial compression strength and splitting strength. The peak strain of the concrete specimens showed a decreasing trend, and the elastic modulus of the concrete was basically unchanged, indicating that a high temperature had an obvious deterioration effect on the concrete, and the deformation ability and strength were reduced gradually.

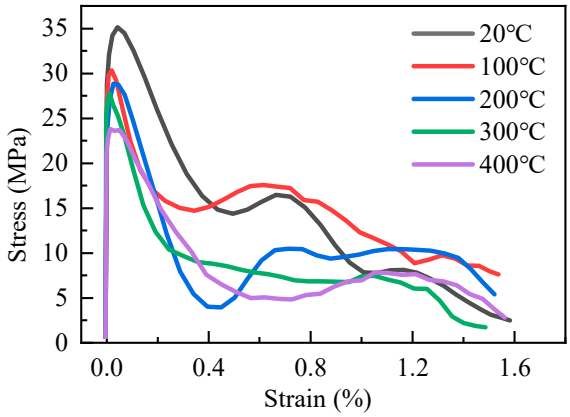

Figure 9. Dynamic stress–strain curve of specimens in dynamic compressive test.

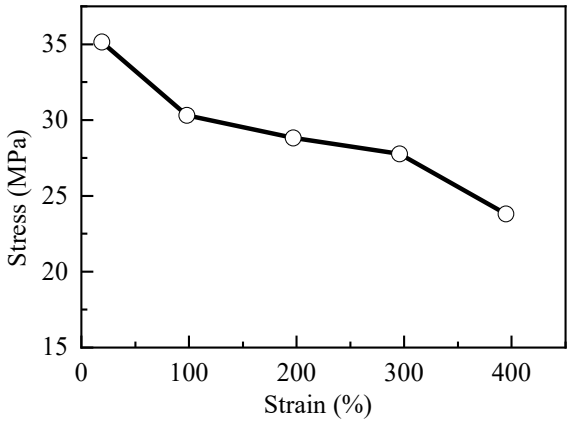

Figure 10. Dynamic compressive strength at different temperature.

3.3. Energy Dissipation Analysis

The energy consumed by the specimen is a comprehensive reflection of the two mechanisms of strength and ductility. The energy dissipation performance of concrete is mainly affected by the external impact energy and internal initial damage state. The external impact energy causes the initiation, development, penetration, and destruction of concrete cracks, which consume a lot of energy. The initial defects formed in the processes of preparation and maintenance of the specimen affect the ability of the specimen to resist the impact load, and then affect the macro-energy performance of the specimen.

The process of the dynamic splitting and failure of the specimens was essentially a process of energy transfer and conversion. Ignoring the energy loss between the rods, the bullet impacted the input bar under high pressure and converted kinetic energy into incident energy, which was transferred in the form of stress waves and finally converted into reflected energy, transmitted energy, and dissipated energy. The formula for calculating the energy carried by the stress wave propagation process in an SHPB test is as follows:

$$W_{\mathrm{I}} = AEC_0 \int \varepsilon_{\mathrm{I}}^2(t)\mathrm{d}t \tag{1}$$

$$W_{\mathrm{R}} = AEC_0 \int \varepsilon_{\mathrm{R}}^2(t)\mathrm{d}t \tag{2}$$

$$W_{\mathrm{T}} = AEC_0 \int \varepsilon_{\mathrm{T}}^2(t)\mathrm{d}t \tag{3}$$

where W_{I} is the incident wave energy, W_{R} is the reflected wave energy, and W_{T} is the transmitted wave energy. $\varepsilon_{\mathrm{I}}(t)$, $\varepsilon_{\mathrm{R}}(t)$, and $\varepsilon_{\mathrm{T}}(t)$ are the incident strain, reflected strain, and transmitted strain at time t, respectively. C_0 is the wave velocity in the bar, A is the cross-sectional area of the press bar, and E is the elastic modulus of the material. Ignoring the energy loss between the bar and the specimen when the stress wave propagates, the dissipated energy of the specimen (W_{s}) is calculated as follows:

$$W_{\mathrm{s}} = W_{\mathrm{I}} - W_{\mathrm{R}} - W_{\mathrm{T}} \tag{4}$$

According to the above formula, the variation law of the dissipated energy of the concrete specimens treated at different temperatures in the dynamic compression test and dynamic splitting test is shown in Figure 11. With the increase in the temperature, the energy absorption value of the samples in the two groups of tests gradually decreased, showing a strong temperature effect. At a high temperature, the cohesiveness and viscoelasticity of the test specimens decreased due to various thermal damages caused by the high temperature, such as the decomposition of gelling products and the weakening of the interface adhesion in the transition zone. The energy absorbed by the specimen for crack

initiation development increased, and the energy dissipation increased. However, as the temperature increased, the strength of the specimen decreased continuously, the absorbed energy became less under the same impact load, and the absorbed energy required for the specimen to achieve failure decreased. Therefore, in the dynamic splitting test and dynamic compression test, the dissipated energy of the specimens decreased with an increase in temperature.

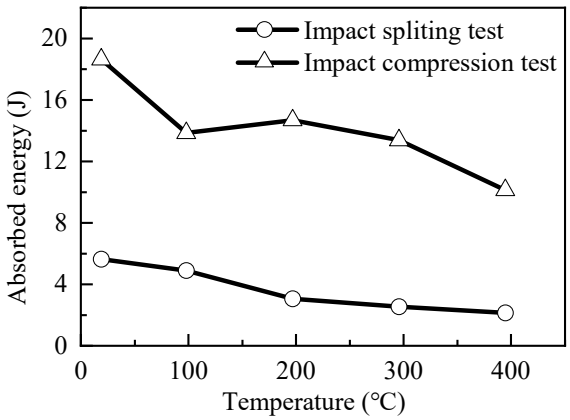

Figure 11. Variation curves of dissipated energy of specimens at different temperatures.

4. Conclusions

In this paper, concrete specimens were treated with different temperatures, and a dynamic splitting test and dynamic compression test were carried out. The progressive failure process of the concrete specimens was studied, the splitting and compression failure modes of the specimens were determined, and the influence mechanism of temperature on the dynamic stress–strain curves and impact resistance of the concrete was revealed. The main conclusions are as follows:

(1) In the impact splitting test, the specimen was first slightly damaged at the loading point, and gradually extended to the core area of the specimen to form a triangular crushing zone. Finally, a penetrating crack was formed in the loading direction, and the specimen was split into two parts. In the impact compression test, the specimen was damaged from the edge and cracks appeared on the surface. The direction of the cracks was consistent with the direction of the loading. With an increase in the load, micro-cracks developed and merged, resulting in the surface block of the specimen falling off, the main crack developing in the core concrete, and the specimen presenting axial splitting failure. After the high-temperature treatment, the specimen showed brittle failure and was finally crushed into fine blocks.

(2) In the impact splitting and impact compression tests, the specimen was in the elastic stage at the initial stage of loading, and quickly reached the peak of the dynamic strength. With an increase in the load, the strength of the specimen decreased sharply, the crack broke through quickly, and the specimen was crushed. After the action of high temperature, the free water and partially bound water inside the concrete produced water vapor pressure, which caused the concrete to be strained and produced micro-cracks and material deterioration, resulting in concrete damage. The dynamic impact resistance of the concrete decreased gradually with the temperature, the toughness of the concrete decreased significantly, and the specimens showed brittle failure in the failure stage. The next steps are to optimize the mix ratio and improve the strength of the sealing wall.

(3) Under impact load, the concrete specimens consumed a lot of energy in the processes of crack initiation, development, penetration, and failure. At a high temperature, the cohesion and viscoelasticity of the specimens decreased due to various thermal damage changes caused by the temperature. The energy of the specimen for crack initiation development increased and the energy dissipation increased. However, the

strength of the specimen decreased continuously with the increase in temperature, the absorbed energy was less under the same impact load, and the absorbed energy required for the specimen to achieve failure decreased. Finally, with the increase in the temperature, the dissipated energy generally showed a decreasing trend.

Author Contributions: Writing—original draft preparation, Q.W.; supervision, Z.L. All authors have read and agreed to the published version of the manuscript.

Funding: The research is supported by the Shaanxi Province Innovative Talent Promotion Plan-Science and Technology Innovation Team (Grant No. 2020TD-021).

Institutional Review Board Statement: Not applicable.

Informed Consent Statement: Not applicable.

Data Availability Statement: Not applicable.

Acknowledgments: We would like to express our sincere gratitude to editor and scholars who diligently reviewed our paper. Their valuable feedback and insightful suggestions have significantly contributed to its substantial improvement.

Conflicts of Interest: The authors declare no conflict of interest.

References

1. Gao, Y.W.; Guo, Z.G.; Zhang, J.; Zheng, B.H. Present situation and prospect of research on prevention and control of thermal disasters in metal mines in China. *Met. Mine* **2022**, *558*, 196–204.
2. Zheng, Z.; Liu, R.T.; Li, S.C.; Zhang, Q.S. Numerical modeling and verification of grouting with mold bag treatment on seepage failure in foundation excavation. *Geomat. Nat. Hazards Risk* **2018**, *9*, 1172–1185. [CrossRef]
3. Zhang, D.; Wang, W.F.; Deng, J.; Wen, H.; Zhai, X. Experimental study and application of LASC foamed concrete to create airtight walls in coal mines. *Adv. Mater. Sci. Eng.* **2020**, *2020*, 6804906. [CrossRef]
4. Yi, X.; Kang, F.R.; Deng, J.; Xiang, Q.; Ma, L. Research and application on inorganic solidified foam filling material for mine. *J. Saf. Sci. Technol.* **2017**, *13*, 136–142.
5. Sun, C.D.; Feng, G.M. Technology of retaining roadway along gob by stowing with high-water-content material. *J. Min. Strata Control Eng.* **2010**, *15*, 58–61.
6. Du, Z.W.; Chen, S.J.; Ma, J.B.; Guo, Z.P.; Yin, D.W. Gob-side entry retaining involving bag filling material for support wall construction. *Sustainability* **2020**, *12*, 6353. [CrossRef]
7. Feng, G.M. Research on the Superhigh-Water Packing Material and Filling Mining Technology and Their Application. Ph.D. Thesis, China University of Mining and Technology, Xuzhou, China, 2019.
8. Yuan, Y. Research on Rapid Building Technology of Mined-Out Area Closed Wall. Master's Thesis, Henan Polytechnic University, Jiaozuo, China, 2017.
9. Bao, X.Q.; Liu, S.; Ma, X.; Gao, L.; Shi, G.Q. Current situation and prospect of mine permanent sealing technology. *Coal Sci. Technol. Mag.* **2022**, *43*, 36–41+46.
10. Yang, S.Q.; Zhong, Y.; Xia, C.B.; Cai, J.W.; Tang, Z.Q.; Liu, J. Experiment study on fire prevention and flame retardant performances of high water backfill material. *Coal Sci. Technol.* **2017**, *45*, 78–83, 179.
11. Qing, S.G.; Qin, W.G.; Ding, P.X.; Wang, Y.M. Model and simulation analysis of fire development and gas flowing influenced by fire zone sealing in coal mine. *Process Saf. Environ. Protect.* **2021**, *149*, 631–642.
12. Zhang, J. Numerical simulation of stress state and stability of closed seal under explosion load. *China Min. Mag.* **2021**, *30*, 121–128.
13. Cheng, J.W.; Zhang, X.X. Damage assessment of mine seal under blast impact load. *China Saf. Sci. J.* **2021**, *31*, 132–137.
14. Liu, F.X. Simulation and Experimental analysis of anti-explosion impact pressure of closed wall in coal mine. *Saf. Coal Mines* **2019**, *50*, 18–21.
15. Bi, J.; Liu, P.F.; Gan, F. Effects of the cooling treatment on the dynamic behavior of ordinary concrete exposed to high temperature. *Constr. Build. Mater.* **2020**, *248*, 118688. [CrossRef]
16. Liu, W.; Mu, C.M.; Liu, J.; Cai, T.Y. Study on static and dynamic mechanical properties of steel fiber self-compacting concrete after heating in a high-temperature. *J. Build. Eng.* **2023**, *73*, 106790. [CrossRef]
17. Xiao, J.Z.; Li, Z.W.; Xie, Q.H.; Shen, L.M. Effect of strain rate on compressive behaviour of high-strength concrete after exposure to elevated temperatures. *Fire Saf. J.* **2016**, *83*, 25–37. [CrossRef]
18. Zhai, C.C.; Chen, L.; Fang, Q.; Chen, W.S.; Jiang, X.Q. Experimental study of strain rate effects on normal weight concrete after exposure to elevated temperature. *Mater. Struct.* **2017**, *50*, 40. [CrossRef]
19. Zhang, C.; Suo, T.; Tan, W.L.; Zhang, X.Y.; Liu, J.J.; Wang, C.X.; Liu, Y.L. An experimental method for determination of dynamic mechanical behavior of materials at high temperatures. *Int. J. Impact Eng.* **2017**, *102*, 27–35. [CrossRef]

20. Chen, C.; Chen, X.D.; Li, X.J. Dynamic compressive behavior of 10-year-old concrete cores after exposure to high temperatures. *J. Mat. Civ. Eng.* **2020**, *32*, 04020076. [CrossRef]
21. Su, H.Y.; Xu, J.Y.; Ren, W.B. Experimental study on the dynamic compressive mechanical properties of concrete at elevated temperature. *Mat. Des.* **2014**, *56*, 579–588. [CrossRef]
22. Li, H.C.; Liu, D.S.; Huang, Y.H.; Liang, S.F.; Li, M.H. Tests for time effect on concrete dynamic mechanical property under high temperature. *J. Vib. Shock* **2015**, *34*, 182–188.
23. Chen, L.; Fang, Q.; Jiang, X.Q.; Ruan, Z.; Hong, J. Combined effects of high temperature and high strain rate on normal weight concrete. *Int. J. Imp. Eng.* **2015**, *86*, 40–56. [CrossRef]
24. Yu, X.; Chen, L.; Fang, Q.; Ruan, Z.; Hong, J.; Xiang, H.B. A concrete constitutive model considering coupled effects of high temperature and high strain rate. *Int. J. Imp. Eng.* **2017**, *101*, 66–77. [CrossRef]
25. Jin, L.; Hao, H.M.; Zhang, R.B.; Du, X.L. Meso-scale simulations of dynamic compressive behavior of concrete at elevated temperature. *Eng. Mech.* **2019**, *36*, 70–78, 118.
26. Jin, L.; Hao, H.M.; Zhang, R.B.; Du, X.L. Meso-scale simulations on dynamic splitting tensile behaviors of concrete at elevated temperatures. *Explos. Shock Waves* **2020**, *40*, 54–65.
27. Li, J.Q.; Zong, Z.H.; Shan, Y.L.; Yu, D.X.; Li, M.H.; Zhao, H. Dynamic compressive behavior of concrete-filled steel tubes under single and multiple impacts. *J. Constr. Steel Res.* **2023**, *208*, 107993. [CrossRef]
28. Wang, Y.T.; Liu, D.S.; Li, S.L.; Jiang, Y.Q. Dynamic performance of concrete based on a Φ75 mm SHPB system under high temperature. *J. Vib. Shock* **2014**, *33*, 12–17.
29. Li, L.; Wang, Z.C.; Wu, J.; Du, X.L.; Wang, H.W.; Liu, W.L. Comparative study on the dynamic mechanical properties of steel fiber reinforced concrete at high temperatures and after high temperature cooling. *Constr. Build. Mater.* **2022**, *346*, 128448. [CrossRef]
30. Zhang, Z.G.; Xu, J.Y.; Su, H.Y.; Liu, Z.Q. Dynamic strength property of concrete at exposure to elevated temperature. *Bull. Chin. Ceram. Soc.* **2015**, *34*, 501–505.
31. Wu, H.S.; Shen, A.Q.; Ren, G.P.; Ma, Q.; Wang, Z. Dynamic mechanical properties of fiber-reinforced concrete: A review. *Constr. Build. Mater.* **2023**, *366*, 130145. [CrossRef]
32. Liu, J.H.; Zhou, Y.C.; Yang, H.T.; Fu, S.F.; Gu, Y. Energy and damage characteristics of shaft lining concrete subjected to impact. *J. China Coal Soc.* **2019**, *44*, 2983–2989.
33. Yang, J.H.; Li, X.Y.; Ye, Y.Q.; Wang, X.Y. Strength and energy dissipation effect of fiber reinforced all-lightweight concrete based on SHPB impact tests. *J. Vib. Shock* **2020**, *39*, 148–153+177.
34. Feng, S.W.; Zhou, Y.; Li, Q.M. Damage behavior and energy absorption characteristics of foamed concrete under dynamic load. *Constr. Build. Mater.* **2022**, *357*, 129340. [CrossRef]
35. Liu, J.; Ren, Y.Z.; Chen, R.; Wu, Y.D.; Lei, W.D. The Effect of Pore Structure on Impact Behavior of Concrete Hollow Brick, Autoclaved Aerated Concrete and Foamed Concrete. *Materials* **2022**, *15*, 4075. [CrossRef] [PubMed]
36. Chao, X.Q. Application of flexible mold inorganic filling material in rapid sealing of roadway. *China Min. Mag.* **2021**, *30*, 66–270.
37. Mohammad, R.K.; Kerstin, W. A review on split Hopkinson bar experiments on the dynamic characterisation of concrete. *Constr. Build. Mater.* **2018**, *190*, 1264–1283.